MEEC/MIEEC

ANALOG INTEGRATED CIRCUITS

Analysis and design of a reference voltage buffer for an ADC

Authors:

Francisco Simões Coelho Sá da Costa (70386) fsc.costa@campus.fct.unl.pt
Martim Duarte Agostinho (70392) md.agostinho@campus.fct.unl.pt
Sofia Margarida Mafra Dias Inácio (58079) sm.inacio@campus.fct.unl.pt

2025/2026 – 1$^{\text{st}}$ Semester, DEEC

Contents

List of Figures

List of Tables

1 Introduction (objectives)

2 AM Communication

2.1 Architecture

2.2 Tests

single tone e musica

3 Digital Communication

For this section two Quadrature Amplitude Modulation (QAM) techniques were used, **Quadrature Phase-Shift Keying (QPSK)** and **16-QAM**. This process involved generating a random stream of bits, modulating them into **QPSK** and **16-QAM** symbols and simulating their transmission through GNU Radio. In the simulation the effects of non-linear Power Amplifier (PA) and Low Noise Amplifier (LNA) were simulated as well as the noise of a Additive White Gaussian Noise (AWGN) channel.

3.1 Digital Modulation

textbfQPSK places four equally spaced points on the unit circle:

$$s_k = e^{j\frac{\pi}{2}\left(k+\frac{1}{2}\right)}, \qquad k \in \{0, 1, 2, 3\}.$$

Figure 1a, shows the mapping in the cartesian plane.

The mapper groups the encoded bit stream into two-bit tuples (b_1, b_0), converts each tuple to an integer index $(k = 2b_1 + b_0)$ and outputs s_k.

The theoretical bit-error probability for QPSK in an AWGN channel is given by Equation 1.

$$P_b^{\text{QPSK}} = Q\left(\sqrt{2\frac{E_b}{N_0}}\right) \; [1] \tag{1}$$

For **QPSK**, demodulation is performed by simply de-mapping the bit values.

With **16-QAM** a 4×4 square constellation was used. What changes comparing to the previous mapping approach is the fact that the amplitude also changes and for this specific mapping the phase and amplitude will not change consistently. The symbol position in the cartesian frame will be:

$$I, R \in \{\pm3, \; \pm1\}$$

For **16-QAM** the theoretical **BER** for an AWGN channel with gray mapping is given by Equation 2.

$$P_b^{\text{16QAM}} \approx \frac{3}{4} \cdot Q\left(\sqrt{\frac{4}{5}\frac{E_b}{N_0}}\right) \; [1] \tag{2}$$

The constellation points are labelled with *Gray coding*, thus every nearest neighbour differs in *exactly one* bit, this will minimize **BER**, since the most likely symbol error produces only one wrong bit. Figure 1b, shows how the codes are mapped.
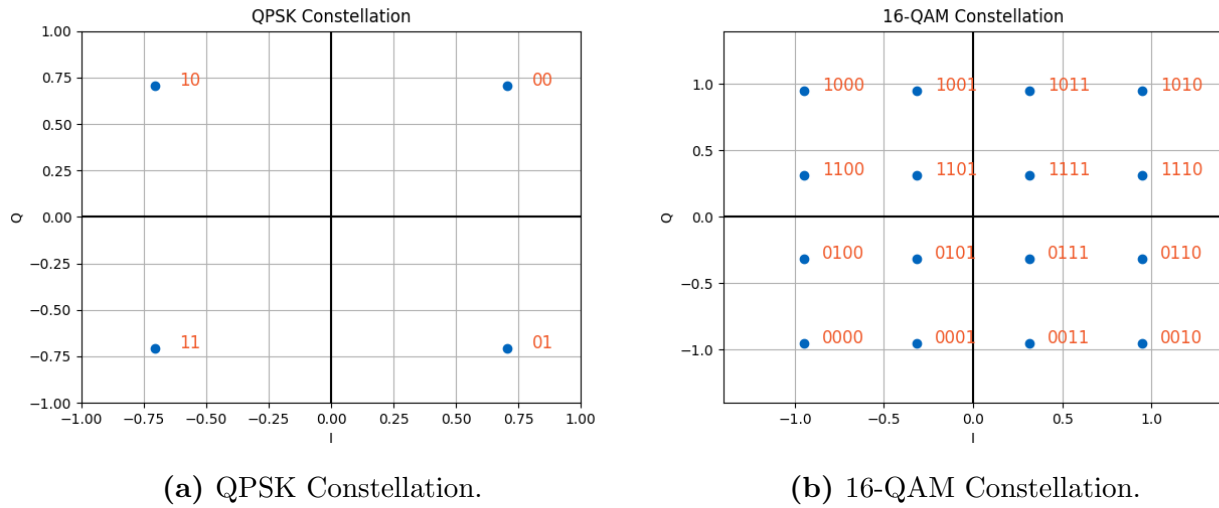

(a) QPSK Constellation.

(b) 16-QAM Constellation.

Figure 1: Digital Modulation Constellations.

3.2 GNU Radio Implementation
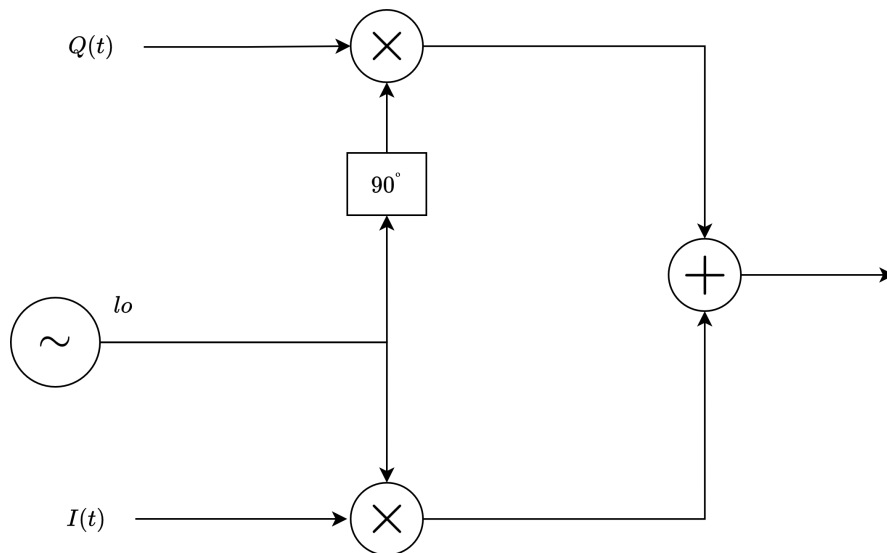
3.2.1 IQ Modulation

INTRO

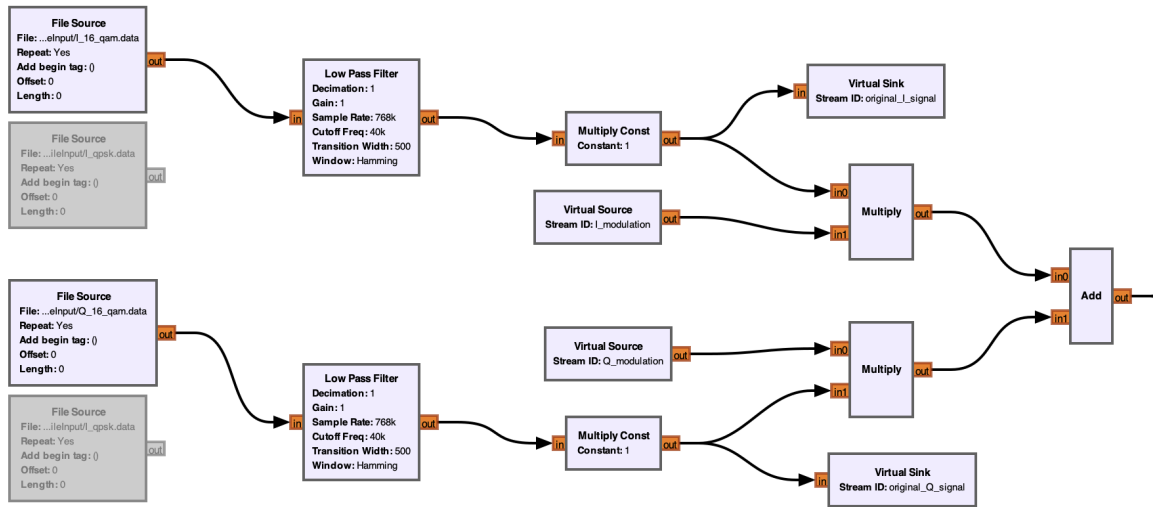
Figure 2: IQ Modulator Block Diagram
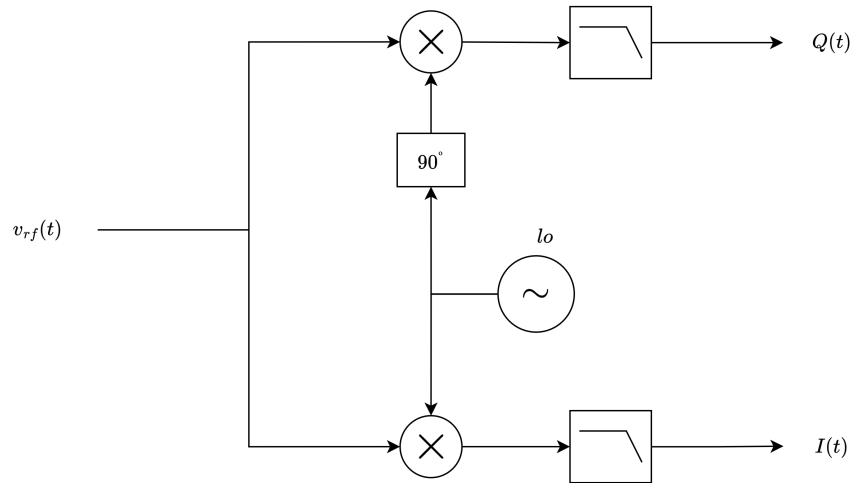
Figure 3: GNU IQ Modulator

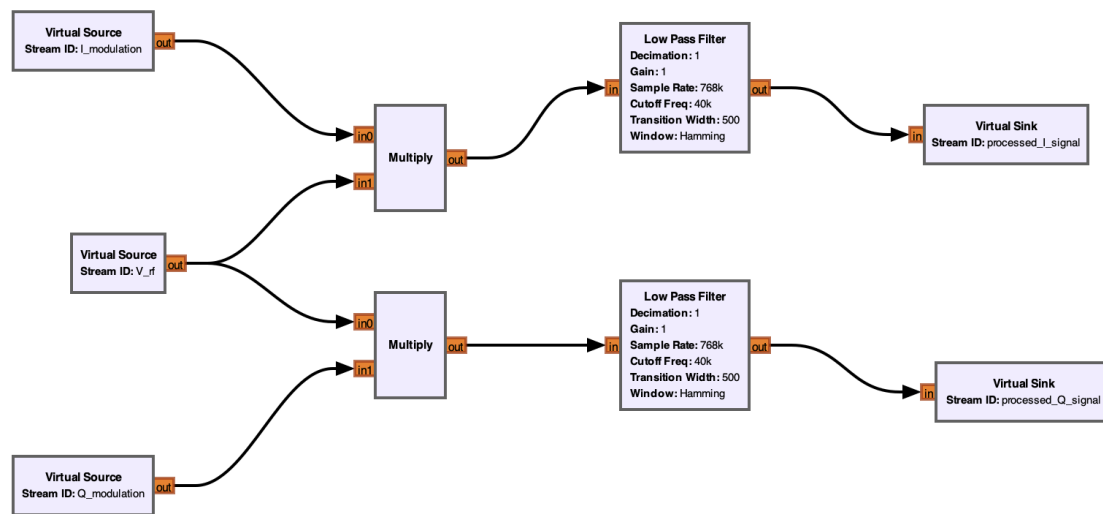**Figure 4:** IQ De-Modulator Block Diagram

Figure 5: GNU IQ De-Modulator

textcolorredArranjar outro titulo e texto a explicar 3 ordem de nao lin, limitacoes que vao apararecer e dizer que pro lNA é mais do mesmo
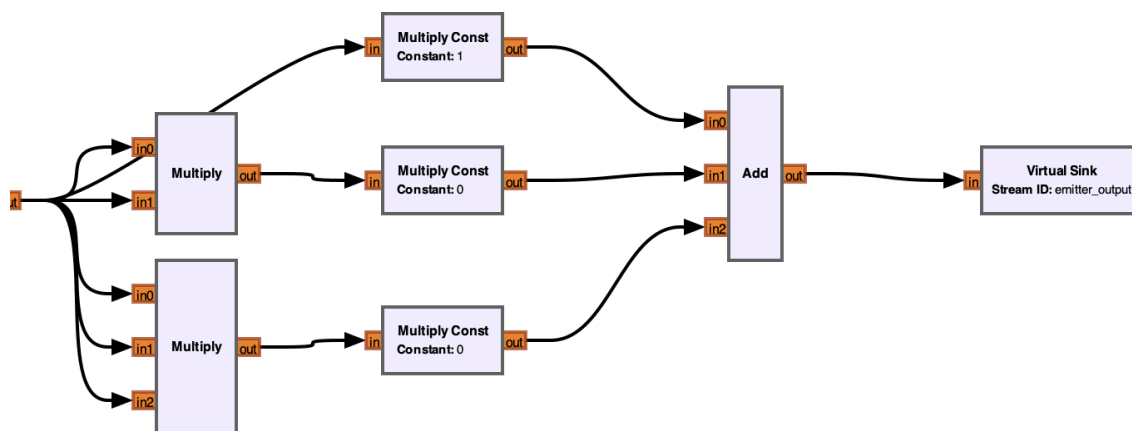

Figure 6: GNU Radio PA non Linear

Dizer que o noise é adicionado antes da atenuaçao para manter o SNR mais facil de quantificar
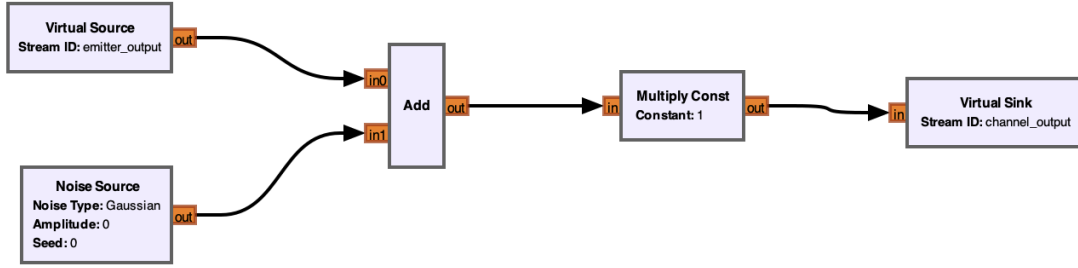
Figure 7: GNU Radio Channel

3.3 Performance Analysis

The primary goal was to evaluate the system's performance by measuring the Bit Error Rate (BER) as a function of the Signal-to-Noise Ratio (SNR) in an AWGN channel.

A random bitstream of 3×10^6 bits was generated using `Gen_symbs.py` Meter cite aos anexos?. This stream was modulated and fed into the GNU Radio simulation. At the receiver, the `Read_Output.py` script was used to read the output files and calculate BER.

Finally with BER values were plotted against the theoretical performance curves, Equations 1 and 2, for both modulation schemes. As shown in Figure 8, in this figure there were no nonlinear effects simulated.
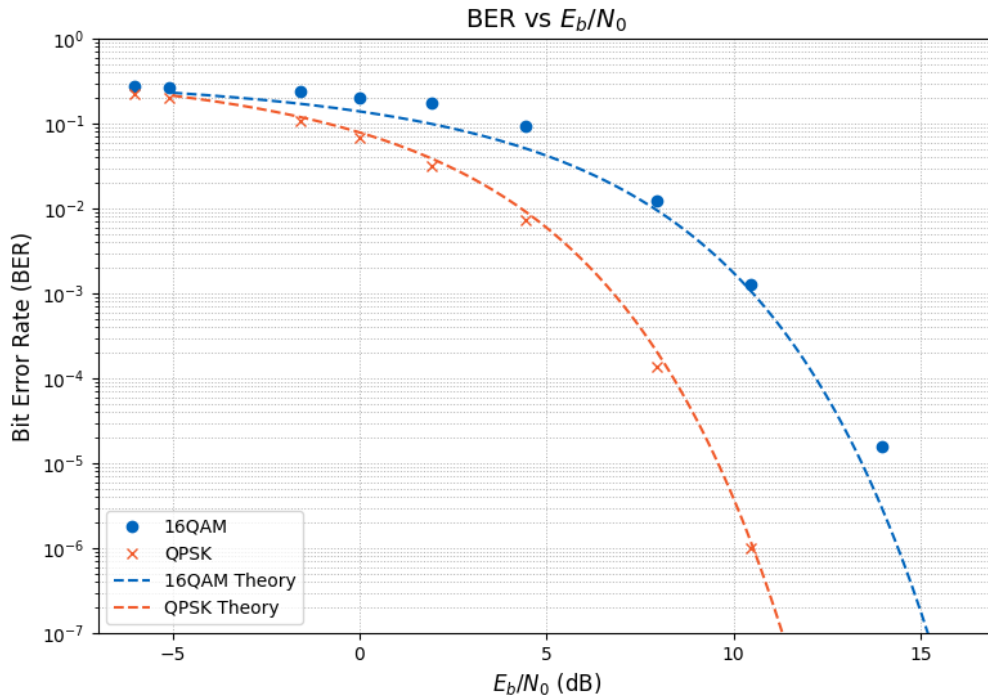

Figure 8: BER vs E_b/N_0

The results in Figure 8 clearly validate our simulation.

QPSK BER points (shown in orange) align almost perfectly with the theoretical QPSK performance curve. This confirms that the simulation chain, including the noise model and demodulator, is functioning correctly.

16-QAM similarly, the simulated 16-QAM data (in Blue) closely follows its theoretical curve.

4 SPICE simulation results and analysis

5 VNA measurements and impedance transformation discussion

6 RFFE experiment setup, results, and analysis

7 Conclusions

References

[1] P. Montezuma, "Transmissão de alta capacidade - topics," 2025, departamento de Engenharia Eletrotécnica, Universidade Nova de Lisboa, FCT.